The Journal of Immunology

Retinoic Acid Signaling in Thymic Epithelial Cells Regulates Thymopoiesis

Kerstin Wendland, Kristoffer Niss, Knut Kotarsky, Nikita Y. H. Wu, Andrea J. White, Johan Jendholm, Aymeric Rivollier, Jose M. G. Izarzugaza, Søren Brunak, Georg A. Holländer, Graham Anderson, Katarzyna M. Sitnik and William W. Agace

J Immunol 2018; 201:524-532; Prepublished online 30 May 2018;
doi: 10.4049/jimmunol.1800418
http://www.jimmunol.org/content/201/2/524

The Journal of Immunology is published twice each month by
The American Association of Immunologists, Inc.,
1451 Rockville Pike, Suite 650, Rockville, MD 20852

Print ISSN: 0022-1767 Online ISSN: 1550-6606.

Retinoic Acid Signaling in Thymic Epithelial Cells Regulates Thymopoiesis

Kerstin Wendland,* Kristoffer Niss,† Knut Kotarsky,* Nikita Y. H. Wu,‡ Andrea J. White,§ Johan Jendholm,‡ Aymeric Rivollier,‡ Jose M. G. Izarzugaza,¶ Søren Brunak,† Georg A. Holländer,‖,# Graham Anderson,§ Katarzyna M. Sitnik,‡ and William W. Agace*,‡

Despite the essential role of thymic epithelial cells (TEC) in T cell development, the signals regulating TEC differentiation and homeostasis remain incompletely understood. In this study, we show a key in vivo role for the vitamin A metabolite, retinoic acid (RA), in TEC homeostasis. In the absence of RA signaling in TEC, cortical TEC (cTEC) and CD80^{lo}MHC class II^{lo} medullary TEC displayed subset-specific alterations in gene expression, which in cTEC included genes involved in epithelial proliferation, development, and differentiation. Mice whose TEC were unable to respond to RA showed increased cTEC proliferation, an accumulation of stem cell Ag-1^{hi} cTEC, and, in early life, a decrease in medullary TEC numbers. These alterations resulted in reduced thymic cellularity in early life, a reduction in CD4 single-positive and CD8 single-positive numbers in both young and adult mice, and enhanced peripheral CD8$^+$ T cell survival upon TCR stimulation. Collectively, our results identify RA as a regulator of TEC homeostasis that is essential for TEC function and normal thymopoiesis. ***The Journal of Immunology*****, 2018, 201: 524–532.**

The generation of functional T cells requires interactions between developing thymocytes and cortical and medullary thymic epithelial cells (TEC) (1). Cortical TEC (cTEC) promote the commitment, expansion, and differentiation of CD4$^-$CD8$^-$ double-negative (DN) thymocytes to CD4$^+$CD8$^+$ double-positive (DP) thymocytes (2) and positive selection of DP thymocytes with TCR specificities able to recognize peptide–MHC complexes (3). In contrast, medullary TEC (mTEC), through their ability to express a broad range of tissue-restricted Ags (3), ensure the elimination of autoreactive TCR specificities within the single-positive (SP) thymocyte pool, are required for the generation of Foxp3$^+$ regulatory T cells, and promote SP thymocyte maturation (4).

Mature cTEC and mTEC originate from a common bipotent progenitor present in both embryonic (5–7) and postnatal (8) thymus via lineage-committed cTEC and mTEC precursor intermediates (9, 10). The environmental signals regulating TEC development and differentiation are incompletely understood but include receptor activator for NF-κB ligand, CD40L, and lymphotoxin derived from developing thymocytes (11) and fibroblast growth factor-7 and -10 (12, 13), and insulin-like growth factor-1 and -2 (14, 15) from thymic mesenchymal cells. We recently found that gp38$^+$ thymic mesenchymal cells produce the vitamin A metabolite, retinoic acid (RA), and that addition of a pan–RA receptor (RAR) antagonist to fetal thymic organ cultures enhances TEC proliferation, which was associated with increased expression of cTEC-lineage genes (16). Although these observations suggest that RA signaling may regulate TEC homeostasis, the in vivo role of RA signaling specifically in TEC in thymic development, homeostasis, and thymopoiesis remains unknown.

RA signals through RAR/retinoid X receptor heterodimers that function as ligand-induced transcription factors binding to RA-responsive elements in the regulatory regions of target genes to regulate gene transcription (17). To investigate the in vivo role of RA signaling in TEC, we generated mice whose TEC express a dominant-negative form of RARα (dnRARα) and are thus unable to respond to RA signals. Our results provide in vivo evidence that RA signaling in TEC regulates postnatal TEC development and expansion with downstream impacts on thymopoiesis.

Materials and Methods

Mice

Foxn1Cre.dnRAR$^{lsl/lsl}$, *dnRAR$^{lsl/lsl}$*, C57BL/6-Tg(TcraTcrb)1100Mjb/J (OT-I), and C57BL/6-Tg(TcraTcrb)425Cbn/J (OT-II) mice were bred and maintained at the Biomedical Center Animal Facility (Lund University).

*Immunology Section, Department of Experimental Medical Science, Lund University, 22184 Lund, Sweden; †Translational Disease Systems Biology Program, Novo Nordisk Foundation Center for Protein Research, Copenhagen University, 2200 Copenhagen, Denmark; ‡Section of Biology and Chemistry, Department for Micro- and Nanotechnology, Technical University of Denmark, 2800 Kongens Lyngby, Denmark; §Institute for Immunology and Immunotherapy, College of Medical and Dental Sciences, Medical School, University of Birmingham, Birmingham B15 2TT, United Kingdom; ¶Integrative Systems Biology Group, Department of Bio and Health Informatics, Technical University of Denmark, 2800 Kongens Lyngby, Denmark; ‖Department of Biomedicine, University Children's Hospital and University of Basel, 4085 Basel, Switzerland; and #Department of Paediatrics, Weatherall Institute of Molecular Medicine, University of Oxford, Oxford OX3 9DU, United Kingdom

ORCIDs: 0000-0001-5910-1525 (K.N.); 0000-0003-3785-0327 (K.K.); 0000-0001-6950-6729 (A.J.W.); 0000-0001-8734-2916 (A.R.); 0000-0003-1754-5122 (J.M.G.I.); 0000-0002-2917-4085 (G.A.).

Received for publication March 20, 2018. Accepted for publication May 7, 2018.

This work was supported by Swedish Natural Science Research Council Grant 621-2013-4048, Danish Medical Research Council Grant DFF-1331-00024, and by funds from the IngaBritt and Arne Lundbergs Foundation. G.A. is supported by Medical Research Council Programme Grant MR/N000919/1 and Cancer Research UK Cancer Immunology Grant CRUK A20753. A.J.W. is supported by Wellcome Trust Seed Award 204375/Z/16/Z.

The sequences presented in this article have been submitted to the National Center for Biotechnology Information Sequence Read Archive (https://www.ncbi.nlm.nih.gov/bioproject/PRJNA454173) under accession number PRJNA454173.

Address correspondence and reprint requests to Prof. William W. Agace, Technical University of Denmark, Henrik Dams Allé, Building 205B, 2800 Kongens Lyngby, Denmark. E-mail address: wiag@vet.dtu.dk

The online version of this article contains supplemental material.

Abbreviations used in this article: cTEC, cortical TEC; DE, differentially expressed; DEG, DE gene; DN, double-negative; dnRARα, dominant-negative form of RARα; DP, double-positive; GO, gene ontology; MHC-II, MHC class II; mTEC, medullary TEC; PCA, principal component analysis; RA, retinoic acid; RAR, RA receptor; RNA-seq, RNA sequencing; RTE, recent thymic emigrant; Sca-1, stem cell Ag-1; SP, single-positive; TEC, thymic epithelial cell; VCT, violet cell tracer.

For thymic injury, mice were injected i.p with dexamethasone (20 mg/kg; Sigma-Aldrich). For in vivo CTL activity, mice were immunized with 1 mg of OVA (grade VI; Sigma-Aldrich) and anti-CD40 (12.5 μg; BioLegend) and injected i.v. 5 d later with violet cell tracer (VCT; Invitrogen)–labeled target (loaded with 0.2 μM OVA, VCT^{lo}) and control cells (VCT^{hi}) at a 1:1 ratio. Mice were sacrificed 4 h postinjection and CTL activity in spleen was calculated as the ratio of target/control cells. All animal procedures were approved by the Lund/Malmö Animal Ethics Committee.

Cell preparation

For TEC analysis, thymus tissue was digested as previously described (16) and TEC were enriched by depleting $CD45^+$ cells with CD45 microbeads (Miltenyi Biotec). For thymocyte and splenocyte analysis, organs were mashed through a 70-μm cell strainer and RBCs lysed using ACK solution.

Flow cytometry analysis and cell sorting

Cells were stained as previously described (16). All analyses were pregated on live singlet cells. Data acquisition was performed on an LSR II (BD Biosciences) and analyzed using FlowJo software (Tree Star). Sorting was performed on a FACSAria II (BD Biosciences). Postsort purity was >95%. For intracellular staining, cells were fixed and permeabilized using a Foxp3 staining buffer set (eBioscience) or 4% paraformaldehyde and 0.1% saponin. CCL21 staining was performed as previously described (18). TCR Vβ usage was assessed using the anti-mouse TCR Vβ screening panel (BD Biosciences). For analysis of BrdU incorporation, mice were injected i.p. with BrdU (1 mg; BD Biosciences), sacrificed after 16 h, and TEC suspensions were stained with FITC-conjugated BrdU (FITC BrdU flow kit; BD Biosciences).

Analysis of thymic sections

Frozen thymic sections were stained with H&E and analyzed as described (19). For confocal microscopy, acetone-fixed thymic sections (7 μm) were stained with rat anti-mouse CD25 (7D4; BD Biosciences), biotinylated rat anti-mouse CD8 (53-5.8; BioLegend), and Alexa Fluor 555–conjugated streptavidin (Life Technologies). Images were acquired on a Zeiss LSM 710 microscope and analyzed using ZEN software (Carl Zeiss MicroImaging).

Quantitative PCR

Indicated samples were analyzed for the presence of the genomic stop cassette using primers neomycin_fw (5′-TGCCGAATATCATGGTGGAAAAT-3′) and neomycin_rev (5′-TCGTCAAGAAGGCGATAGAAGGCG-3′) and compared with the presence of the dnRAR construct. Expression of dnRAR was assessed using primers dnRAR_fw (5′-GACTGCAGAAGTGCTTTGAA-3′) and dnRAR_rev (5′-GCACTCGGGCTTGGGCA-3′) using Kapa SYBR Fast quantitative PCR master mix (Kapa Biosystems). In all cases, mRNA levels were normalized to β-actin.

T cell stimulation

Naive splenic T cells were incubated (5×10^4 cells per well) on anti-CD3 (145-2C11; Bio X Cell) precoated U-bottom 96-well plates with or without soluble anti-CD28 (37.51, 1 μg/ml; Bio X Cell) at 37°C and 5% CO_2. Thymidine (1 μCi [^{3}H]thymidine; PerkinElmer) was added after 48 h, and 18 h later cells were harvested with a cell harvester (Tomtec). [^{3}H]thymidine was assessed on a 1450 MicroBeta TriLux (PerkinElmer). For assessing proliferation, cells were VCT labeled prior to incubation and harvested after 66 h. For Ca^{2+} flux, cells (4×10^6) were loaded with Fluo-4 (7 μM; Life Technologies) and Fura Red (35 μM; Molecular Probes) and incubated with anti-CD3 (10 mg/ml, 145-2C11; Bio X Cell) for 10 min at 37°C. Crosslinking Ab (1–20 μg, goat anti–Armenian hamster IgG; Jackson ImmunoResearch Laboratories) was added and Ca^{2+} flux monitored on a FACSAria II for 250 s.

RNA sequencing

RNA was prepared using an RNeasy Micro Kit (Qiagen) and amplified using an Ovation RNA-Seq System V2 (NuGEN) kit. cDNA libraries, generated with an Ovation Ultralow System V2 kit (NuGEN), were fragmented using a Bioruptor Pico (Diagenode) and sheared cDNA end repaired to generate blunt ends, ligated to Illumina adaptors with indexing tags, and purified using AMPure XP beads. Libraries were sequenced on a HiSeq 2500 System (Illumina) using 150-bp paired-end reads (Center for Biological Sequence Analysis, Technical University of Denmark, Copenhagen, Denmark). Sample reads were aligned to the mouse Ensembl genome assembly using HISAT-2 (version 2.0.1), and expression counts were quantified using htseq-count. For normalization, gene expression data of each sample were combined in R and genes with <25 counts in two samples within a single condition were excluded. Principal component analysis (PCA) was performed using the R function prcomp and PCA plots were generated using ggplot2. The R package Limma was used for differentially expressed (DE) analysis. Genes with a q value < 0.05 (Benjamini–Hochberg) were considered significant. The complete sets of DE genes (DEG) were tested for gene ontology (GO) biological process enrichment using gProfileR (version 0.6.1) (20). Heat maps were created using gplots function heatmap.2. RNA sequencing (RNA-seq) data were deposited in the National Center for Biotechnology Information Sequence Read Archive (https://www.ncbi.nlm.nih.gov/bioproject/PRJNA454173) under accession number PRJNA454173.

Statistical analysis

All statistical analyses apart from RNA-seq experiments were performed using GraphPad Prism 7.0. Statistical analysis was performed using unpaired two-tailed Student t test. A p value < 0.05 was considered significant ($*p < 0.05$, $**p < 0.01$, $***p < 0.001$, $****p < 0.0001$).

Results

Adult mice whose TEC cannot respond to RA display enhanced numbers of cTEC

To investigate the role of RA signaling in TEC in vivo, *dnRAR*$^{lsl/lsl}$ mice (21) that carry a *lox*P-flanked stop cassette preceding the coding sequence for a dnRARα (RARα403), previously used to assess the role of RA signaling in hematopoietic cells (22, 23), were crossed with *Foxn1Cre* mice (24) to generate *Foxn1Cre*.*dnRAR*$^{lsl/lsl}$ mice. Deletion of the stop cassette in TEC from *Foxn1Cre*.*dnRAR*$^{lsl/lsl}$ mice (hereafter termed Cre^+) but not *dnRAR*$^{lsl/lsl}$ littermates (hereafter termed Cre^-) was confirmed at the genomic level by quantitative PCR (Fig. 1A), which resulted in expression of dnRAR by these cells (Fig. 1B).

Adult (8 wk) Cre^+ and Cre^- littermates showed similar thymic architecture, including cortical and medullary size (Supplemental Fig. 1A, 1B). However, quantitative flow cytometry analysis demonstrated a significant increase in cTEC numbers in both female and male Cre^+ mice (Fig. 1C, 1D), whereas $CD80^{lo}$ MHC class II $(MHC\text{-}II)^{lo}$ mTEC ($mTEC^{lo}$) and $CD80^{hi}MHC\text{-}II^{hi}$ mTEC ($mTEC^{hi}$) as well as proportions of AIRE or CCL21 expressing mTEC were unchanged (Fig. 1D, Supplemental Fig. 1C). Thus, RA signaling in TEC appears to be required for cTEC homeostasis in adult mice.

RA regulates numerous distinct biological pathways in cTEC and mTEC^{lo} subsets

To further understand the role of RA signaling in TEC biology, cTEC, $mTEC^{lo}$, and $mTEC^{hi}$ were sorted in triplicate from 8-wk-old Cre^+ and Cre^- littermates, and their gene expression profiles were assessed by RNA-seq. PCA confirmed reproducibility between the datasets and clearly separated cTEC, $mTEC^{lo}$, and $mTEC^{hi}$ subsets (Fig. 2A). Only four genes were DE in $mTEC^{hi}$ between Cre^+ and Cre^- mice (data not shown, q value < 0.05, Benjamini–Hochberg FDR), indicating that RA signaling has little impact on these cells. In contrast, 382 genes in cTEC and 408 genes in $mTEC^{lo}$ were identified as DE between Cre^+ and Cre^- mice (Fig. 2B, 2C). Only 81 DEG were shared by cTEC and $mTEC^{lo}$, indicating that most direct or indirect RA-controlled genes are regulated in a TEC subset–specific manner (Fig. 2C).

GO enrichment analysis of the DEG for cTEC and $mTEC^{lo}$ demonstrated significantly enriched GO terms for epithelial cell proliferation and epithelial cell differentiation in cTEC (Fig. 2D) whereas those for $mTEC^{lo}$ included processes of secretion, cell adhesion, and ion transport (Fig. 2E).

Impaired RA signaling in TEC results in increased cTEC proliferation

Given the enhanced cTEC numbers in adult Cre^+ mice (Fig. 1D) and the RA-regulated GO term related to epithelial cell proliferation in cTEC (Figs. 2D, 3A, 3B), we assessed TEC proliferation in adult

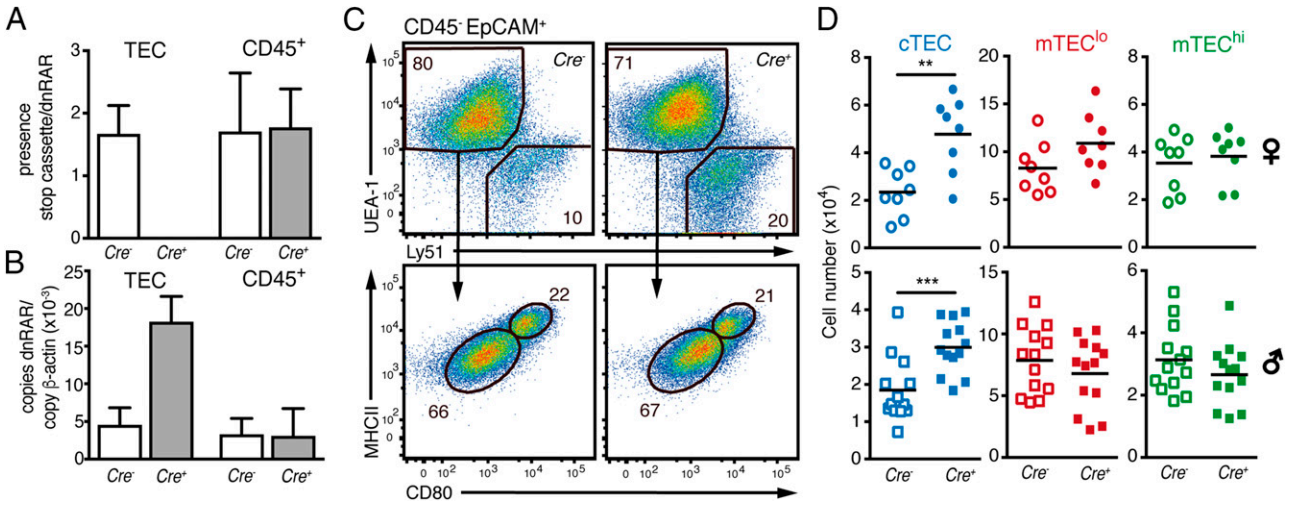

FIGURE 1. Adult *Foxn1Cre.dnRAR*$^{lsl/lsl}$ mice have increased numbers of cTEC. (**A**) Presence of the genomic STOP cassette and (**B**) relative expression of dnRAR mRNA in sorted TEC and CD45$^+$ thymocytes from Cre$^-$ (open bar) and Cre$^+$ (filled bar) mice. Fold levels represent the mean (SD) of (A) four and (B) five biological replicates. (**C**) Representative flow cytometry plots and (**D**) total number of cTEC (UEA-1$^-$Ly51$^+$), mTEC^{lo} (UEA-1$^+$Ly51$^-$CD80^{lo} MHC-II^{lo}), and mTEC^{hi} (UEA-1$^+$Ly51$^-$CD80^{hi}MHC-II^{hi}) subsets (pregating: live single CD45$^-$EpCAM$^+$) from female (♀) and male (♂) Cre$^-$ and Cre$^+$ mice. Data are from three experiments. $^{**}p < 0.01$, $^{***}p < 0.001$. EpCAM, epithelial cell adhesion molecule; UEA-1, *Ulex europeaus* agglutinin-1.

Cre$^+$ and Cre$^-$ littermates. Sixteen hours after BrdU injection cTEC, but not mTEC, from Cre$^+$ mice showed increased BrdU incorporation compared with cTEC from Cre$^-$ mice (Fig. 3C, Supplemental Fig. 1D). Thus, enhanced cTEC proliferation may contribute, at least in part, to the increased numbers of cTEC in adult Cre$^+$ mice.

Impaired RA signaling in TEC results in increased numbers of stem cell Ag-1^{hi} cTEC and reduced numbers of mTEC during postnatal TEC expansion

The identification of RA-regulated GO terms related to epithelial development and differentiation in Cre$^+$ cTEC (Figs. 2D, 4A, 4B) prompted us to investigate alterations in TEC in early life, during the period of TEC expansion (25). The Ly51$^+$ cTEC compartment of adult mice contains bipotent TEC progenitors (9, 26), and stem cell Ag-1 (Sca-1) has been implicated as a marker that is enriched in cells with bipotent progenitor potential (9, 26). We thus assessed surface expression of Sca-1 within the cTEC compartment over time. Cre$^+$ mice had a significant increase in Sca-1^{hi} cTEC numbers from birth into adulthood compared with Cre$^-$ littermates, whereas Sca-1^{lo} cTEC numbers were comparable (Fig. 4C, 4D). Furthermore, Cre$^+$ mice had reduced numbers of mTEC during the first 3 wk of life (Fig. 4E), a time period where

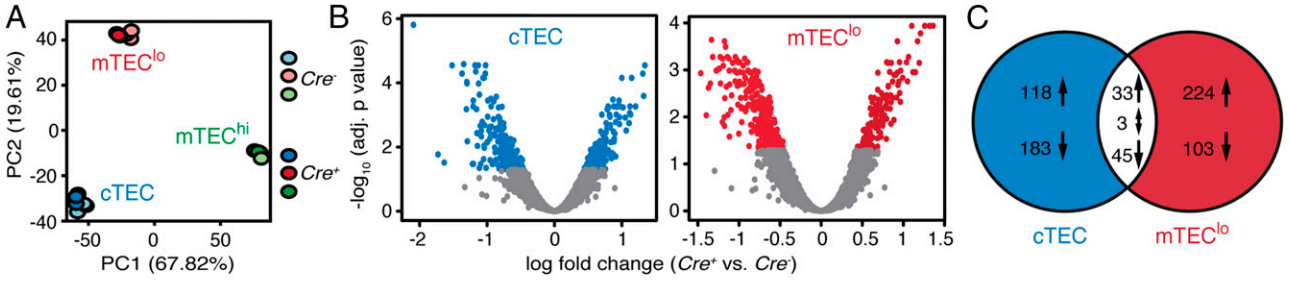

D List of significant GO terms - cTEC

Gene Ontology term	p value	# DEG
System process	1.93×10^{-8}	62
Multicellular organismal process	4.50×10^{-8}	184
Epithelial cell proliferation	2.22×10^{-6}	26
Anatomical structure development	7.70×10^{-5}	151
Developmental process	2.19×10^{-4}	158
Extracellular matrix organisation	7.08×10^{-4}	16
Cell adhesion	1.46×10^{-3}	55
Epithelium development	3.91×10^{-3}	41
Cell differentiation	4.31×10^{-3}	106
Epithelial cell differentiation	5.18×10^{-3}	26

E List of significant GO terms - mTEC^{lo}

Gene Ontology term	p value	# DEG
System process	3.62×10^{-9}	66
G-protein coupled receptor signaling pathway	4.30×10^{-7}	38
Signaling	9.21×10^{-7}	164
Cell communication	6.03×10^{-6}	162
Secretion by cell	1.29×10^{-5}	42
Cell adhesion	2.21×10^{-5}	63
Regulation of biological quality	3.62×10^{-5}	110
Signal transduction	1.18×10^{-4}	145
Regulation of ion transmembrane transport	1.97×10^{-3}	21
Immune response	2.03×10^{-2}	42

FIGURE 2. Altered gene expression in TEC from *Foxn1Cre.dnRAR*$^{lsl/lsl}$ mice. Comparative gene expression analysis of TEC subsets from 8-wk-old Cre$^-$ and Cre$^+$ mice. cTEC, mTEC^{lo}, and mTEC^{hi} subsets were sorted in three experiments from five to six pooled female mice per experiment. (**A**) PCA of all TEC subsets and (**B**) volcano plots showing DEG in Cre$^+$ versus Cre$^-$ mice from RNA-seq analysis of cTEC and mTEC^{lo} subsets. DE (FDR < 0.05, colored dots) and non-DE (gray dots) are shown. (**C**) Venn diagram of DEG in indicated TEC subsets from Cre$^+$ mice. ↑, upregulated in the absence of RA signaling; ↓, downregulated in the absence of RA signaling; ↕, downregulated in one TEC subset but upregulated in the other. (**D** and **E**) Lists of most significant GO terms in cTEC (D) and mTEC^{lo} (E) from Cre$^+$ mice.

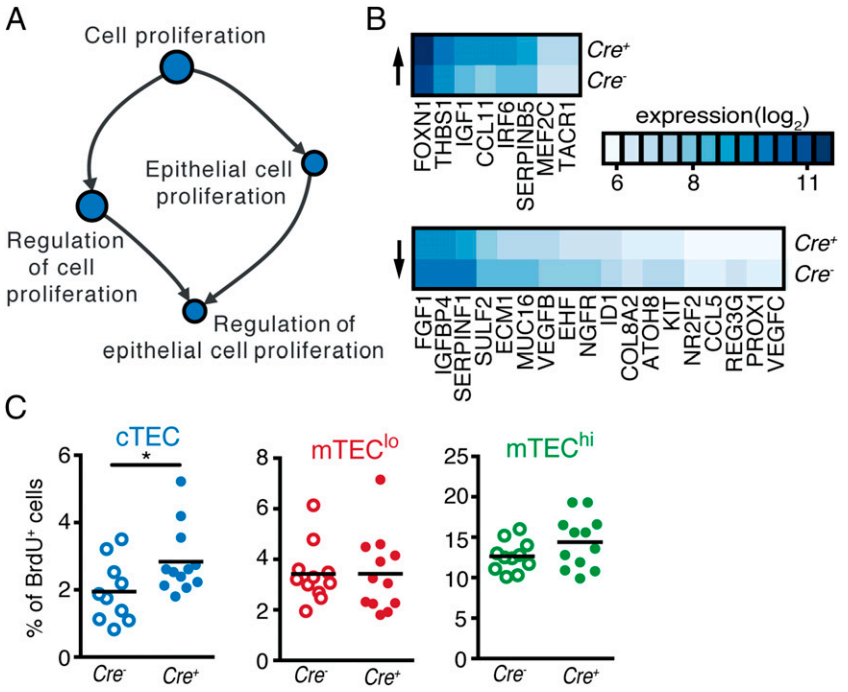

FIGURE 3. Increased proliferation of cTEC in *Foxn1Cre.dnRAR*$^{lsl/lsl}$ mice. (**A**) Cell proliferation GO term network and (**B**) heat maps of DEG in the epithelial cell proliferation GO term. ↑, upregulated in the absence of RA signaling; ↓, downregulated in the absence of RA signaling. Circle size is relative to number of DEG in GO term. (**C**) Percentage of BrdU$^+$ cells in indicated TEC subsets 16 h postinjection. Data are from three experiments. $*p < 0.05$.

mTEC derive primarily from bipotent progenitors displaying a cTEC-specific phenotype (27–30). These results demonstrate that RA signaling modulates cTEC/mTEC ratios in early life, potentially by regulating the ability of bipotent cTEC-like progenitors to give rise to mTEC.

Increased TEC regeneration after thymic injury in the absence of RA signaling

To investigate the role of RA signaling in TEC during thymic regeneration, 8-wk-old Cre$^+$ mice and Cre$^-$ littermates were injected i.p with a single dose of dexamethasone (31). Such treatment results in rapid thymus involution, followed by an extended recovery phase (32). In line with the above studies, dexamethasone treatment resulted in a dramatic reduction in thymocyte and TEC numbers 2 d postinjection (Fig. 5). Thymocyte as well as mTEC^{lo} and mTEC^{hi} numbers were significantly lower in Cre$^+$ compared with Cre$^-$ mice (Fig. 5A, 5C), whereas cTEC loss remained the same between both groups (Fig. 5B). In contrast, during the recovery phase 12 d postinjection, cTEC and mTEC^{lo} numbers were significantly higher in Cre$^+$ mice compared with Cre$^-$ littermates, despite similar levels of thymocyte restoration (Fig. 5). Thus, RA signaling in TEC appears to influence TEC recovery during injury-induced thymic regeneration.

RA signaling in TEC impacts conventional T cell development

Given the importance of TEC in T cell development, we next assessed the impact of RA signaling in TEC on thymopoiesis. Cre$^+$ mice had reduced thymic cellularity from 1 d to 5 wk after birth compared with Cre$^-$ littermates (Fig. 6A), whereas adult Cre$^+$ mice displayed normal thymocyte cellularity (Fig. 6A). Young (12-d-old) Cre$^+$ mice had reduced numbers of DN, DP, and SP thymocytes (Fig. 6B). Among DN subsets, DN3 and DN4, but not ETP or DN2 numbers, were reduced (Supplemental Fig. 2A), whereas localization of CD25$^+$ thymocytes, which in the outer cortex and subcapsular zone almost exclusively represent DN2 and DN3 thymocytes (33), to the subcapsular zone appeared normal (Fig. 6C). Total DP numbers were similar in 5- and 8-wk-old Cre$^+$ and Cre$^-$ mice (Fig. 6B); however, numbers of CD69^{int}TCRβ^{int} DP (DP^{int}) and CD69^{hi} TCRβ^{hi} DP (DP^{hi}), which represent minor DP subpopulations undergoing and immediately subsequent to positive selection (34, 35), were reduced in Cre$^+$ mice at 5 (Fig. 6D, 6E) but not 8 wk (data not shown). CD4SP and CD8SP numbers were reduced in Cre$^+$ mice at all analyzed time points (Fig. 6B), including both immature CD24^{hi}CD62L^{lo} and mature CD24^{lo}CD62L^{hi} SP subsets (Supplemental Fig. 2C, 2D). Expression of TEC genes previously implicated in regulating thymocyte development and survival did not differ between Cre$^+$ and Cre$^-$ mice (Supplemental Fig. 2E, 2F).

Finally, the proportions of Foxp3$^+$ cells among CD4SP thymocytes and numbers of γδ T cells, NKT cells, and intraepithelial lymphocyte precursors (36) were similar between Cre$^+$ and Cre$^-$ mice (Supplemental Fig. 2G–L). Taken together, these results suggest that in the absence of RA signaling in TEC, the generation of conventional CD4SP and CD8SP thymocytes is moderately impaired.

Normal positive selection in mice that lack RA signaling in TEC

The reduction in postselection DP and SP subsets in Cre$^+$ mice prompted us to determine whether the absence of RA signaling in TEC impacted positive selection. Cre$^+$ and Cre$^-$ mice were backcrossed onto a TCR transgenic OT-I and OT-II background to assess selection in the setting of a fixed monoclonal TCR repertoire, allowing for detection of subtle changes in thymocyte selection (37, 38). Similar frequencies of OT-I CD8SP and OT-II CD4SP were found in Cre$^+$ and Cre$^-$ mice (Fig. 7A, Supplemental Fig. 3A). Additionally, CD5 expression on DP thymocytes, as a measure of TCR signaling strength (39), was similar in Cre$^+$ and Cre$^-$ mice (Fig. 7B). Finally, the overall TCR repertoire of CD4SP and CD8SP thymocytes, as assessed by flow cytometry analysis of Vβ gene usage, was similar in Cre$^+$ and Cre$^-$ mice, although we did observe significant alterations in the gene usage of Vβ2 and Vβ5.1/5.2 in CD8SP thymocytes (Supplemental Fig. 3B). Collectively, these findings suggest that RA signaling in TEC does not impact positive selection in a major way.

RA signaling in TEC is not required for thymic egress of mature thymocytes

Given the reduction in SP thymocytes, we next assessed the peripheral T cell compartment of Cre$^+$ mice. The total number of naive

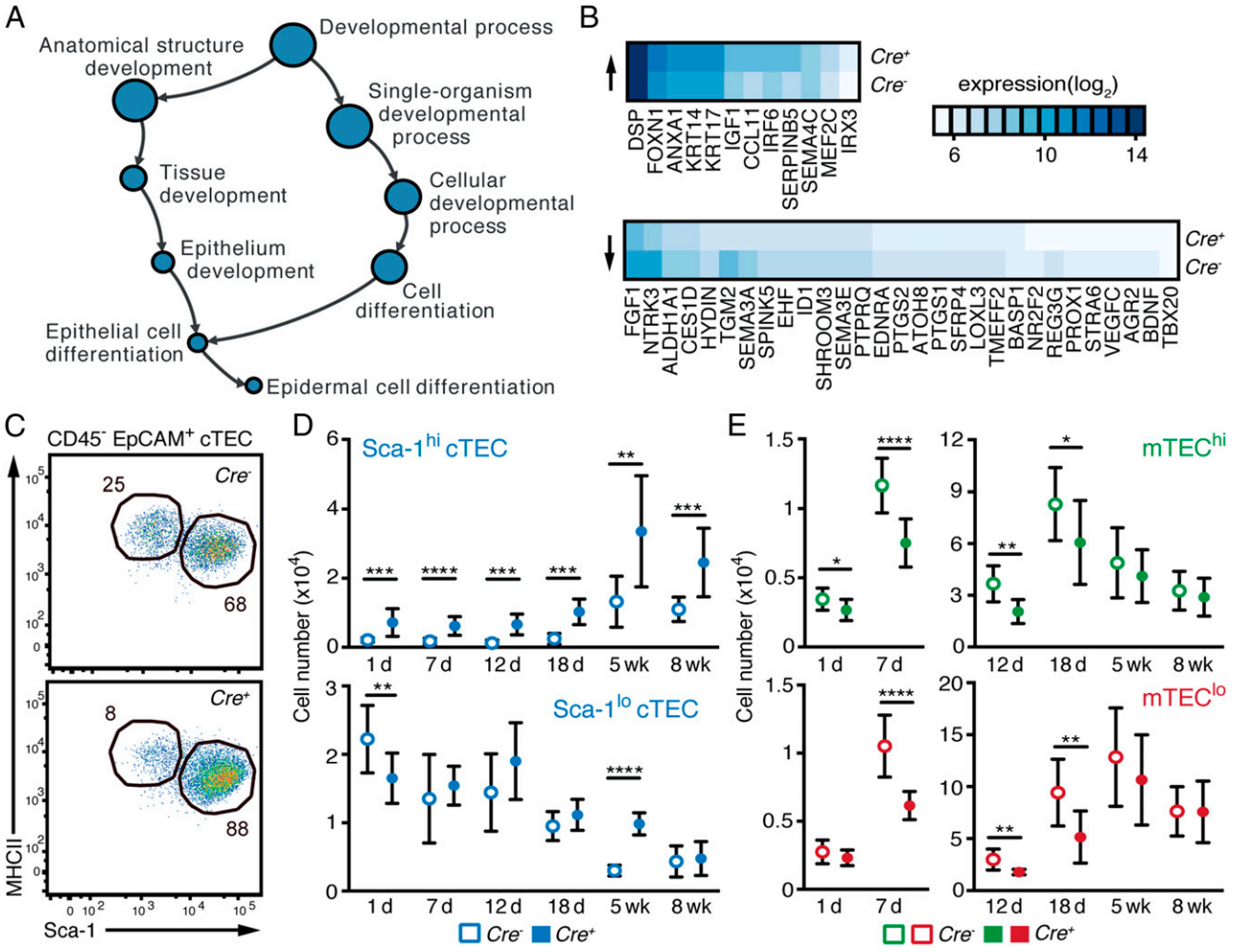

FIGURE 4. Distinct developmental kinetics of TEC and increase of Sca-1^{hi} cTEC in *Foxn1Cre.dnRAR*$^{lsl/lsl}$ mice. (**A**) Developmental process GO term network and (**B**) heat maps of DEG in the epithelium development GO term. ↑, upregulated in the absence of RA signaling; ↓, downregulated in the absence of RA signaling. Circle size is relative to number of DEG in GO term. (**C**) Representative flow cytometry plots of Sca-1^{hi} and Sca-1^{lo} cTEC and (**D** and **E**) total number of indicated TEC subsets over time. Mean (SD) of three experiments with three to six mice per time point and experiment. $*p < 0.05$, $**p < 0.01$, $***p < 0.001$, $****p < 0.0001$.

(CD62L^{hi}CD44^{lo}) CD4$^+$ and CD8$^+$ splenic T cells did not differ between 8-wk-old Cre$^+$ and Cre$^-$ littermates (Fig. 7C). Given that recent thymic emigrants (RTEs) represent only a minor subset of the naive T cell pool in adult mice (40), we next assessed thymic egress in irradiated Cre$^+$ and Cre$^-$ littermates reconstituted with bone marrow cells from Rag2p-GFP mice (41). GFP signal in these mice peaks in DP thymocytes and remains detectable 1−2 wk after cessation of Rag expression, thus allowing for the identification of GFP$^+$ RTEs in the periphery (41). The frequencies of GFP$^+$ RTEs among naive splenic CD4$^+$ and CD8$^+$ T cells and GFP expression levels on RTEs did not differ between Cre$^+$ and Cre$^-$ BM chimeras (Fig. 7D, Supplemental Fig. 3C, 3D). Additionally, surface expression of CD24 and Qa2, markers used to discriminate RTEs from the mature naive T cell pool (41), was similar in unmanipulated Cre$^+$ and Cre$^-$ mice (Fig. 7E, 7F). Taken together, these results suggest that the absence of RA signaling in TEC does not impact SP thymocyte residence time in the medulla or thymic egress.

Impaired RA signaling in TEC alters the response of naive CD8$^+$ T cells to TCR stimulation

Finally, to assess whether the absence of RA signaling in TEC impacted peripheral naive T cell functionality, sorted splenic naive CD4$^+$ and CD8$^+$ T cells from Cre$^+$ and Cre$^-$ mice were stimulated with anti-CD3 or anti-CD3/anti-CD28 and their proliferation was assessed by thymidine incorporation (Fig. 8A, 8B). CD8$^+$ T cells from Cre$^+$ mice incorporated thymidine to a greater extent than did their Cre$^-$ counterparts over a wide range of anti-CD3 concentrations (Fig. 8B).

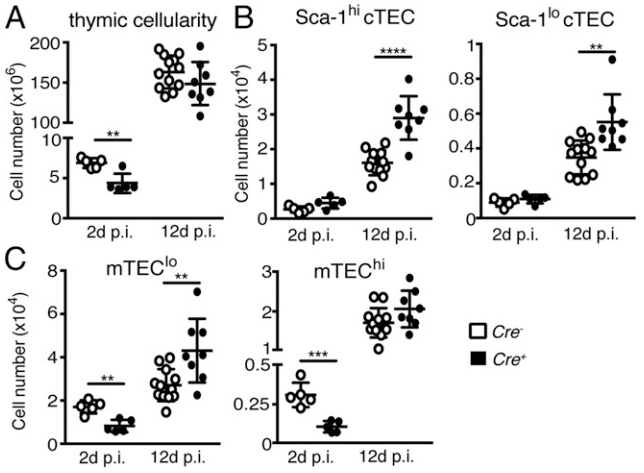

FIGURE 5. Enhanced TEC regeneration in *Foxn1Cre.dnRAR*$^{lsl/lsl}$ mice upon glucocorticoid-induced thymic injury. (**A**–**C**) Impact of glucocorticoid-induced thymic injury on (A) thymic cellularity, (B) Sca-1^{hi} or Sca-1^{lo} cTEC, and (C) mTEC^{lo} and mTEC^{hi} numbers. Data are from two experiments. $**p < 0.01$, $***p < 0.001$, $****p < 0.0001$.

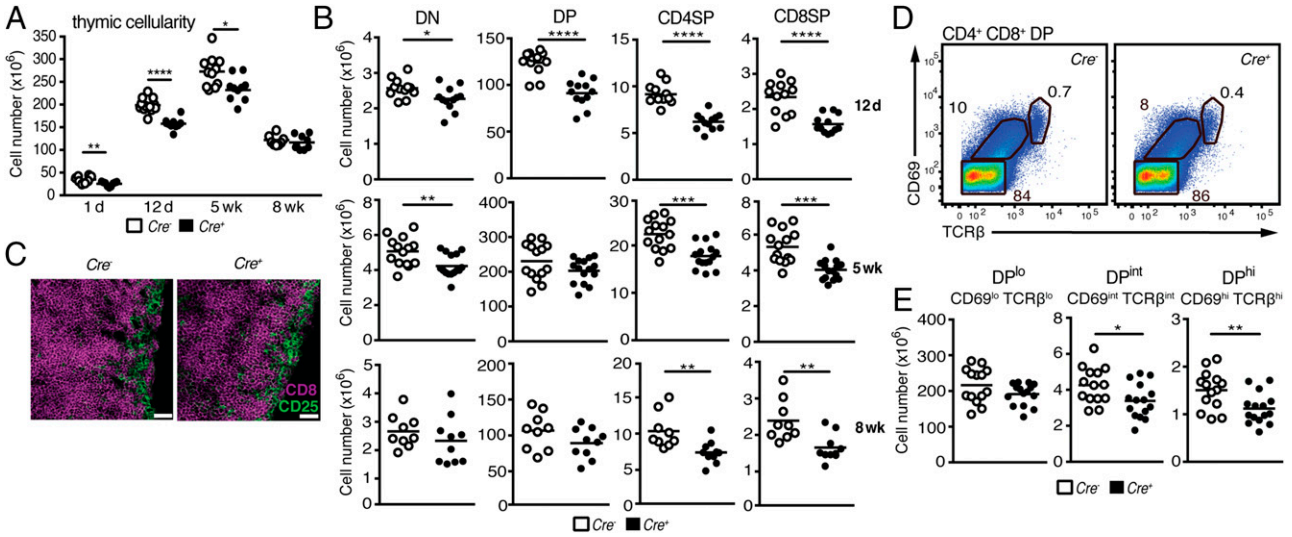

FIGURE 6. *Foxn1Cre.dnRAR$^{lsl/lsl}$* mice display reduced thymic cellularity in early life and maintain decreased SP numbers into adulthood. (**A**) Thymic cellularity and (**B**) total number of DN ($CD4^-CD8^-$), DP ($CD4^+CD8^+$), CD4SP ($CD4^+CD8^-$), and CD8SP ($CD4^-CD8^+$) thymocytes at indicated time points. Data are from (A) three to five or (B) three experiments. (**C**) Confocal images of thymus sections of 12-d-old mice stained for CD25 (green) and CD8 (purple). Images are representative of four mice per strain. Scale bars, 100 μm. (**D**) Representative flow cytometry plots and (**E**) total number of DP subsets before (DP^{lo}), during (DP^{int}) and after selection (DP^{hi}) in 5-wk-old mice. Data are from three experiments. $*p < 0.05$, $**p < 0.01$, $***p < 0.001$, $****p < 0.0001$.

Consistent with this, more $CD8^+$ T cells were recovered from anti-CD3 and anti-CD3/anti-CD28 cultures when cells originated from Cre^+ mice (Fig. 8C). In contrast, induction of CD69 (Fig. 8D, Supplemental Fig. 4A), calcium flux in response to anti-CD3 stimulation across a range of crosslinking Ab concentrations (Fig. 8E, data not shown), and cellular division assessed by VCT dilution (Supplemental Fig. 4B, 4C) were similar in $CD8^+$ T cells from Cre^+ and Cre^- mice. Finally, OVA and anti-CD40 immunized Cre^+ and Cre^- mice displayed a similar ability to kill OVA-pulsed target cells in vivo (Fig. 8F, 8G), indicating that $CD8^+$ T cells from Cre^+ mice are capable of differentiating into functional CTL. Collectively, these results suggest that although naive $CD8^+$ T cells show enhanced survival following anti-CD3 stimulation in vitro, their ability to respond to anti-CD3 and to differentiate into functional CTL appears normal.

Discussion

In this study, we assessed the impact of RA signaling in TEC for TEC and thymocyte development in vivo. Our results confirm and extend our previous in vitro observations in fetal thymic organ cultures (16) that inhibition of RA signaling enhances cTEC expansion. Additionally, we show that the absence of RA signaling alters the expression of numerous, yet largely nonoverlapping, genes in cTEC and $mTEC^{lo}$, with DEG in cTEC associated with epithelial cell proliferation and development. In the absence of RA signaling in TEC, immature Sca-1^{hi} cTEC numbers increased whereas mTEC numbers decreased during early postnatal thymic expansion, resulting in reduced thymopoiesis. Inhibition of RA signaling in TEC also led to reduced SP numbers, and naive $CD8^+$ T cells generated under these conditions displayed increased survival following anti-CD3 stimulation in vitro. Collectively, our results suggest that RA signaling in TEC in vivo is required for normal TEC development and function.

Lack of RA signaling in TEC had little impact on the gene expression profile of $mTEC^{hi}$, indicating that mature $mTEC^{hi}$ in vivo are not exposed to or are unresponsive to RA. In contrast, significant changes were observed in the gene expression profiles of cTEC and $mTEC^{lo}$. DEG between cTEC and $mTEC^{lo}$ were largely nonoverlapping, consistent with previous studies in embryonic fibroblasts and stem cells (42),

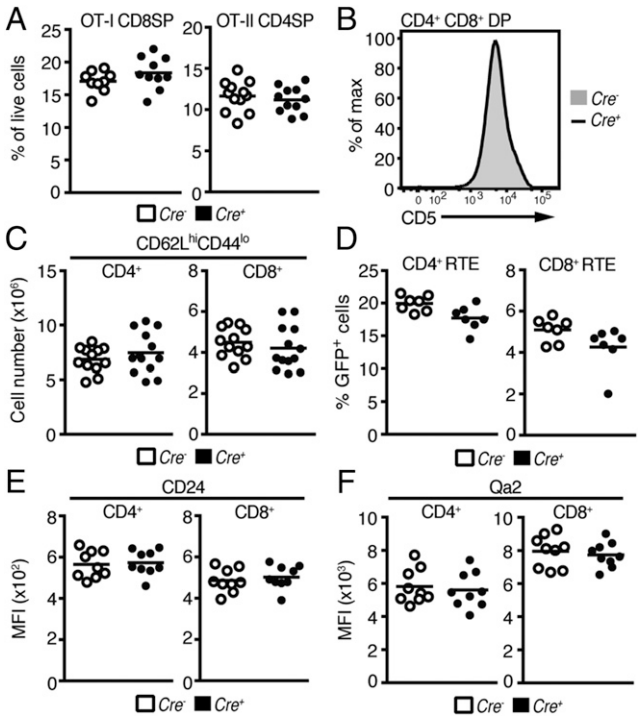

FIGURE 7. Normal positive selection and thymic egress in *Foxn1Cre.dnRAR$^{lsl/lsl}$* mice. (**A**) Percentage of CD8SP or CD4SP cells of live thymocytes in Cre^- (○) and Cre^+ (●) OT-I and OT-II mice. (**B**) CD5 expression of DP thymocytes. Data are representative of two experiments with four mice per group and experiment. (**C**) Total number of splenic naive $CD4^+$ and $CD8^+$ cells. (**D**) Frequencies of GFP^+ RTE within splenic naive ($CD62L^{hi}CD44^{lo}$) $CD4^+$ and $CD8^+$ T cells in mice reconstituted with Rag2pGFP bone marrow and (**E** and **F**) mean fluorescence intensity (MFI) of (E) CD24 and (F) Qa2 expression on naive splenic $CD4^+$ and $CD8^+$ T cells. Data are from three (A and C) or two (D–F) experiments.

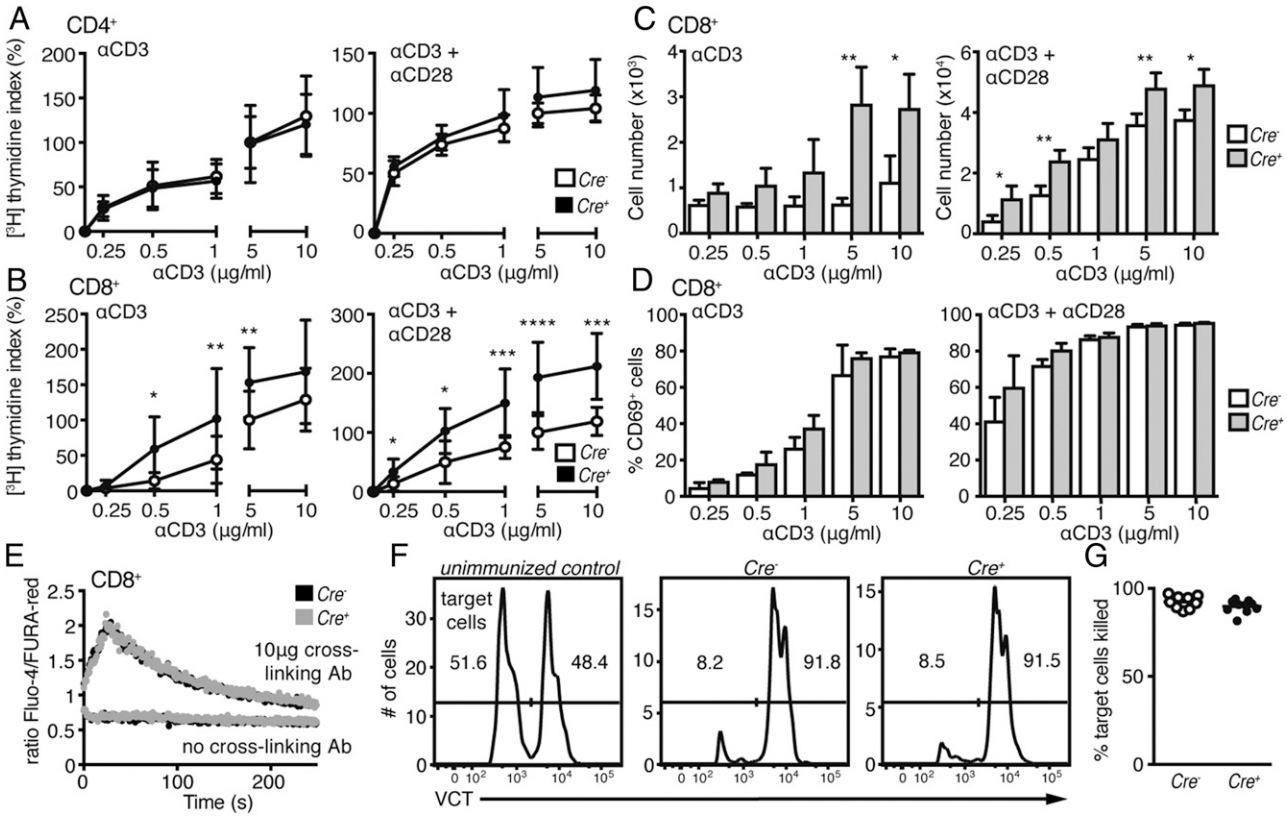

FIGURE 8. Increased numbers of naive CD8$^+$ T cells from *Foxn1Cre.dnRAR$^{lsl/lsl}$* mice following anti-CD3 stimulation in vitro. (**A** and **B**) [^{3}H]thymidine incorporation of anti-CD3– or anti-CD3/anti-CD28–stimulated naive (A) CD4$^+$ or (B) CD8$^+$ T cells. Mean (SD) of three experiments with four mice per group and anti-CD3 condition in each experiment. Results were normalized between experiments by setting the mean cpm for Cre$^-$ at 5 μg/ml anti-CD3 to 100% for each experiment (cpm counts for the three experiments: CD4$^+$, 89,942, 58,209, 233,127; CD8$^+$, 89,513, 38,643, 43,635). (**C**) Total number of CD8$^+$ T cells and (**D**) frequencies of CD8$^+$CD69$^+$CD62L^{lo} T cells after indicated stimulation. Mean (SD) of four mice per group and anti-CD3 condition in each experiment. (**E**) Ca^{2+} response of naive splenic CD8$^+$ T cells to anti-CD3 stimulation. Data are representative of two experiments with four mice per group. (**F**) Representative flow cytometry plots mice and (**G**) percentage of killed target cells 4 h postinjection into OVA and anti-CD40–immunized mice. Data are from three experiments. $*p < 0.05$, $**p < 0.01$, $***p < 0.001$, $****p < 0.0001$.

suggesting that gene regulation by RA is highly cell type specific. Indeed, the biological processes controlled by RA in cTEC but not mTEC^{lo} included cell development and differentiation, GO terms previously identified to be overrepresented in cTEC when compared with mTEC (43). Which proportion of these DEG are direct RA targets or regulated indirectly by RA through the regulation of, for example, transcription factors, nuclear receptors, or histone-modifying enzymes (44) is difficult to assess using current technologies given limitations in TEC numbers.

GO analysis of DEG in cTEC in the absence of RA signaling predicted alterations in epithelial cell proliferation and included upregulation of FOXN1 and insulin-like growth factor-1, known drivers of TEC proliferation (11), indicating a potential role for RA signaling in limiting cTEC cycling. Consistent with this, as well as our prior in vitro studies (16), we observed that cTEC but not mTEC proliferation was increased in the absence of RA signaling. This increase in proliferation likely contributes, at least in part, to the increased numbers of cTEC observed in Cre$^+$ mice, although we cannot exclude additional effects.

Consistent with the GO analysis predicting alterations in epithelial differentiation, absence of RA signaling in TEC resulted in increased numbers of Sca-1^{hi} cTEC, which in early postnatal life was associated with decreased numbers of mTEC. mTEC derive from bipotent progenitors that bear a cTEC phenotype during embryonic and early postnatal thymic expansion (27, 28, 45), and Sca-1^{hi} cTEC have previously been described to contain bipotent progenitors in the postnatal thymus (9, 26). Thus, although the identity of bipotent progenitors within the postnatal cTEC compartment remains unknown, our results indicate that RA signaling in such progenitors may serve to promote mTEC development. Although the underlying direct or indirect RA-regulated genes, or sets of genes, responsible for these alterations remain unclear, these results are in line with the role of RA in regulating the differentiation of intestinal epithelial transit amplifying progenitors into secretory and enteroendocrine cells in vivo (46) and various epithelial cell lines in vitro (47, 48). Future experiments assessing the gene expression profile and turnover of Sca-1^{hi} and Sca-1^{lo} cTEC subsets in Cre$^+$ and Cre$^-$ mice may help identify potential additional roles of RA in cTEC development from bipotent precursors.

In contrast to early postnatal life, mTEC in adult mice are maintained through mTEC-restricted progenitors (10, 30, 49). Cre$^+$ mice showed a normalization of mTEC numbers with age when mice transition to an adult mTEC developmental program, indicating that RA may promote the differentiation of mTEC from bipotent, but not mTEC-restricted, precursors. The full recovery of mTEC numbers in adult Cre$^+$ mice further suggests that RA signaling may confer a proliferative or survival advantage for mTEC-committed cells. In support of this, we found enhanced restoration of mTEC numbers in the

absence of RA signaling following thymic injury, a process driven by mTEC-committed precursors (49).

In the absence of RA signaling in TEC we observed age-dependent alterations in thymopoiesis, with a significant reduction in DN, DP, and SP thymocytes at 12 d of age, which became restricted to SP thymocytes with age. At 12 d, ETP and DN2 numbers appeared normal in Cre$^+$ mice whereas DN3 numbers were reduced, indicating that RA signaling in TEC is not required for thymic seeding, but potentially provides an optimal environment for DN3 survival and development. RA deficiency impairs expression of the Notch ligand Delta-like 1 in the embryonic spinal cord (50). Although expression of the Notch ligand Delta-like 4, a key factor for survival and differentiation of DN3 thymocytes (51), was similar in 8-wk-old Cre$^+$ and Cre$^-$ mice, further analysis of the transcriptional profile of cTEC from 12-d-old Cre$^+$ and Cre$^-$ mice might shed light on why DN3 thymocyte numbers are reduced at this age. Finally, although reduced DN3 numbers in 12-d-old Cre$^+$ mice may partially underlie the reduction in subsequent thymocyte subsets, mature thymocyte numbers were more significantly reduced at this age, indicating potential additional roles of RA signaling in TEC in early thymopoiesis.

Total DP thymocyte numbers recovered with age in Cre$^+$ mice, potentially as a result of niche filling; however, postselection DP subsets were reduced at 5 wk of age whereas SP thymocyte numbers remained reduced in adults. Although we cannot rule out subtle changes in the selecting peptide repertoire, our results indicate that positive selection is largely unaffected in Cre$^+$ mice. However, alterations in the gene usage of several Vβ gene families might suggest minor effects on the resulting TCR repertoire, the significance of which remains to be determined. The reduced numbers of SP thymocytes in Cre$^+$ mice appear not to be due to alterations in thymic egress or SP maturation. Moreover, expression of TEC genes previously implicated in thymopoiesis did not differ between Cre$^+$ and Cre$^-$ mice. We thus speculate that mTEC of Cre$^+$ mice, despite normal numbers, are qualitatively less capable of supporting SP thymocyte survival or, alternatively, induce stronger negative selection. Such effects are likely mediated by as yet unidentified RA-regulated genes or sets of genes impacting TEC–thymocyte interactions or through alterations in niche availability.

A final finding from our studies was that absence of RA signaling in TEC impacted naive CD8$^+$ T cells. Despite normal numbers in vivo, naive splenic CD8$^+$ T cells from Cre$^+$ mice incorporated more thymidine following anti-CD3 stimulation in vitro. Anti-CD3–induced calcium flux, CD69 expression and proliferation, and the in vivo CTL activity of CD8$^+$ T cells from Cre$^+$ and Cre$^-$ mice were similar, indicating normal responsiveness to TCR stimulation. In contrast, the number of CD8$^+$ T cells recovered from anti-CD3 cultures was higher when cells originated from Cre$^+$ mice. A possible explanation for these findings is that T cell development within an RA signaling–deficient TEC environment alters the threshold by which CD8$^+$ T cells undergo activation-induced cell death, perhaps through inhibition of Nur77 or its family members, known to induce TCR-mediated apoptosis during negative selection but also in mature T cells (52). Analysis of signaling pathways downstream of the TCR, as well as assessment of primary and recall CD8$^+$ T cell responses in Cre$^+$ and Cre$^-$ mice, should help elucidate the extent to which RA signaling deficiency in TEC impacts peripheral T cell function.

In summary, in this study, we identify RA signaling in TEC as a key regulator of TEC homeostasis and function. Future studies focusing on the identification of direct and indirect RA target genes in TEC subsets should help provide a better understanding of the molecular mechanisms underlying these findings.

Acknowledgments

We thank Dr. Julien Vandamme (Technical University of Denmark) and Dr. Kirstine G. Belling (University of Copenhagen, Copenhagen, Denmark) for technical support and Ann-Charlotte Selberg (Lund University) for animal care and genotyping.

Disclosures

The authors have no financial conflicts of interest.

References

1. Anderson, G., and Y. Takahama. 2012. Thymic epithelial cells: working class heroes for T cell development and repertoire selection. *Trends Immunol.* 33: 256–263.
2. Nitta, T., and H. Suzuki. 2016. Thymic stromal cell subsets for T cell development. *Cell. Mol. Life Sci.* 73: 1021–1037.
3. Takaba, H., and H. Takayanagi. 2017. The mechanisms of T cell selection in the thymus. *Trends Immunol.* 38: 805–816.
4. Takahama, Y., I. Ohigashi, S. Baik, and G. Anderson. 2017. Generation of diversity in thymic epithelial cells. *Nat. Rev. Immunol.* 17: 295–305.
5. Bennett, A. R., A. Farley, N. F. Blair, J. Gordon, L. Sharp, and C. C. Blackburn. 2002. Identification and characterization of thymic epithelial progenitor cells. *Immunity* 16: 803–814.
6. Gill, J., M. Malin, G. A. Holländer, and R. Boyd. 2002. Generation of a complete thymic microenvironment by MTS24$^+$ thymic epithelial cells. *Nat. Immunol.* 3: 635–642.
7. Rossi, S. W., W. E. Jenkinson, G. Anderson, and E. J. Jenkinson. 2006. Clonal analysis reveals a common progenitor for thymic cortical and medullary epithelium. *Nature* 441: 988–991.
8. Bleul, C. C., T. Corbeaux, A. Reuter, P. Fisch, J. S. Mönting, and T. Boehm. 2006. Formation of a functional thymus initiated by a postnatal epithelial progenitor cell. *Nature* 441: 992–996.
9. Ulyanchenko, S., K. E. O'Neill, T. Medley, A. M. Farley, H. J. Vaidya, A. M. Cook, N. F. Blair, and C. C. Blackburn. 2016. Identification of a bipotent epithelial progenitor population in the adult thymus. *Cell Rep.* 14: 2819–2832.
10. Sekai, M., Y. Hamazaki, and N. Minato. 2014. Medullary thymic epithelial stem cells maintain a functional thymus to ensure lifelong central T cell tolerance. *Immunity* 41: 753–761.
11. Abramson, J., and G. Anderson. 2017. Thymic epithelial cells. *Annu. Rev. Immunol.* 35: 85–118.
12. Revest, J. M., R. K. Suniara, K. Kerr, J. J. T. Owen, and C. Dickson. 2001. Development of the thymus requires signaling through the fibroblast growth factor receptor R2-IIIb. *J. Immunol.* 167: 1954–1961.
13. Dooley, J., M. Erickson, W. J. Larochelle, G. O. Gillard, and A. G. Farr. 2007. FGFR2IIIb signaling regulates thymic epithelial differentiation. *Dev. Dyn.* 236: 3459–3471.
14. Chu, Y. W., S. Schmitz, B. Choudhury, W. Telford, V. Kapoor, S. Garfield, D. Howe, and R. E. Gress. 2008. Exogenous insulin-like growth factor 1 enhances thymopoiesis predominantly through thymic epithelial cell expansion. *Blood* 112: 2836–2846.
15. Jenkinson, W. E., S. W. Rossi, S. M. Parnell, E. J. Jenkinson, and G. Anderson. 2007. PDGFRα-expressing mesenchyme regulates thymus growth and the availability of intrathymic niches. *Blood* 109: 954–960.
16. Sitnik, K. M., K. Kotarsky, A. J. White, W. E. Jenkinson, G. Anderson, and W. W. Agace. 2012. Mesenchymal cells regulate retinoic acid receptor-dependent cortical thymic epithelial cell homeostasis. *J. Immunol.* 188: 4801–4809.
17. Rochette-Egly, C., and P. Germain. 2009. Dynamic and combinatorial control of gene expression by nuclear retinoic acid receptors (RARs). *Nucl. Recept. Signal.* 7: e005.
18. Sitnik, K. M., K. Wendland, H. Weishaupt, H. Uronen-Hansson, A. J. White, G. Anderson, K. Kotarsky, and W. W. Agace. 2016. Context-dependent development of lymphoid stroma from adult CD34$^+$ adventitial progenitors. *Cell Rep.* 14: 2375–2388.
19. Cosway, E. J., B. Lucas, K. D. James, S. M. Parnell, M. Carvalho-Gaspar, A. J. White, A. V. Tumanov, W. E. Jenkinson, and G. Anderson. 2017. Redefining thymus medulla specialization for central tolerance. *J. Exp. Med.* 214: 3183–3195.
20. Reimand, J., T. Arak, P. Adler, L. Kolberg, S. Reisberg, H. Peterson, and J. Vilo. 2016. g:Profiler—a web server for functional interpretation of gene lists (2016 update). *Nucleic Acids Res.* 44: W83–W89.
21. Rajaii, F., Z. T. Bitzer, Q. Xu, and S. Sockanathan. 2008. Expression of the dominant negative retinoid receptor, RAR403, alters telencephalic progenitor proliferation, survival, and cell fate specification. *Dev. Biol.* 316: 371–382.
22. Allie, S. R., W. Zhang, C. Y. Tsai, R. J. Noelle, and E. J. Usherwood. 2013. Critical role for all-*trans* retinoic acid for optimal effector and effector memory CD8 T cell differentiation. *J. Immunol.* 190: 2178–2187.
23. Pantazi, E., E. Marks, E. Stolarczyk, N. Lycke, R. J. Noelle, and R. Elgueta. 2015. Cutting edge: retinoic acid signaling in B cells is essential for oral immunization and microflora composition. *J. Immunol.* 195: 1368–1371.
24. Jeker, L. T., T. Barthlott, M. P. Keller, S. Zuklys, M. Hauri-Hohl, C. X. Deng, and G. A. Holländer. 2008. Maintenance of a normal thymic microenvironment

and T-cell homeostasis require Smad4-mediated signaling in thymic epithelial cells. *Blood* 112: 3688–3695.
25. Gray, D. H., N. Seach, T. Ueno, M. K. Milton, A. Liston, A. M. Lew, C. C. Goodnow, and R. L. Boyd. 2006. Developmental kinetics, turnover, and stimulatory capacity of thymic epithelial cells. *Blood* 108: 3777–3785.
26. Wong, K., N. L. Lister, M. Barsanti, J. M. Lim, M. V. Hammett, D. M. Khong, C. Siatskas, D. H. Gray, R. L. Boyd, and A. P. Chidgey. 2014. Multilineage potential and self-renewal define an epithelial progenitor cell population in the adult thymus. *Cell Reports* 8: 1198–1209.
27. Ohigashi, I., S. Zuklys, M. Sakata, C. E. Mayer, S. Zhanybekova, S. Murata, K. Tanaka, G. A. Holländer, and Y. Takahama. 2013. Aire-expressing thymic medullary epithelial cells originate from β5t-expressing progenitor cells. *Proc. Natl. Acad. Sci. USA* 110: 9885–9890.
28. Baik, S., E. J. Jenkinson, P. J. Lane, G. Anderson, and W. E. Jenkinson. 2013. Generation of both cortical and Aire$^+$ medullary thymic epithelial compartments from CD205$^+$ progenitors. *Eur. J. Immunol.* 43: 589–594.
29. Alves, N. L., Y. Takahama, I. Ohigashi, A. R. Ribeiro, S. Baik, G. Anderson, and W. E. Jenkinson. 2014. Serial progression of cortical and medullary thymic epithelial microenvironments. [Published erratum appears in 2014 *Eur. J. Immunol.* 44: 2197.] *Eur. J. Immunol.* 44: 16–22.
30. Mayer, C. E., S. Žuklys, S. Zhanybekova, I. Ohigashi, H. Y. Teh, S. N. Sansom, N. Shikama-Dorn, K. Hafen, I. C. Macaulay, M. E. Deadman, et al. 2016. Dynamic spatio-temporal contribution of single β5t$^+$ cortical epithelial precursors to the thymus medulla. *Eur. J. Immunol.* 46: 846–856.
31. Fletcher, A. L., T. E. Lowen, S. Sakkal, J. J. Reiseger, M. V. Hammett, N. Seach, H. S. Scott, R. L. Boyd, and A. P. Chidgey. 2009. Ablation and regeneration of tolerance-inducing medullary thymic epithelial cells after cyclosporine, cyclophosphamide, and dexamethasone treatment. *J. Immunol.* 183: 823–831.
32. Talaber, G., K. Kvell, Z. Varecza, F. Boldizsar, S. M. Parnell, E. J. Jenkinson, G. Anderson, T. Berki, and J. E. Pongracz. 2011. Wnt-4 protects thymic epithelial cells against dexamethasone-induced senescence. *Rejuvenation Res.* 14: 241–248.
33. Liston, A., K. M. Nutsch, A. G. Farr, J. M. Lund, J. P. Rasmussen, P. A. Koni, and A. Y. Rudensky. 2008. Differentiation of regulatory Foxp3$^+$ T cells in the thymic cortex. *Proc. Natl. Acad. Sci. USA* 105: 11903–11908.
34. Swat, W., M. Dessing, H. von Boehmer, and P. Kisielow. 1993. CD69 expression during selection and maturation of CD4$^+$8$^+$ thymocytes. *Eur. J. Immunol.* 23: 739–746.
35. Yamashita, I., T. Nagata, T. Tada, and T. Nakayama. 1993. CD69 cell surface expression identifies developing thymocytes which audition for T cell antigen receptor-mediated positive selection. *Int. Immunol.* 5: 1139–1150.
36. Ruscher, R., R. L. Kummer, Y. J. Lee, S. C. Jameson, and K. A. Hogquist. 2017. CD8αα intraepithelial lymphocytes arise from two main thymic precursors. *Nat. Immunol.* 18: 771–779.
37. Jenkinson, W. E., K. Nakamura, A. J. White, E. J. Jenkinson, and G. Anderson. 2012. Normal T cell selection occurs in CD205-deficient thymic microenvironments. *PLoS One* 7: e53416.
38. Mingueneau, M., W. Jiang, M. Feuerer, D. Mathis, and C. Benoist. 2012. Thymic negative selection is functional in NOD mice. *J. Exp. Med.* 209: 623–637.
39. Azzam, H. S., A. Grinberg, K. Lui, H. Shen, E. W. Shores, and P. E. Love. 1998. CD5 expression is developmentally regulated by T cell receptor (TCR) signals and TCR avidity. *J. Exp. Med.* 188: 2301–2311.
40. Hale, J. S., T. E. Boursalian, G. L. Turk, and P. J. Fink. 2006. Thymic output in aged mice. *Proc. Natl. Acad. Sci. USA* 103: 8447–8452.
41. Boursalian, T. E., J. Golob, D. M. Soper, C. J. Cooper, and P. J. Fink. 2004. Continued maturation of thymic emigrants in the periphery. *Nat. Immunol.* 5: 418–425.
42. Delacroix, L., E. Moutier, G. Altobelli, S. Legras, O. Poch, M. A. Choukrallah, I. Bertin, B. Jost, and I. Davidson. 2010. Cell-specific interaction of retinoic acid receptors with target genes in mouse embryonic fibroblasts and embryonic stem cells. *Mol. Cell. Biol.* 30: 231–244.
43. St-Pierre, C., S. Brochu, J. R. Vanegas, M. Dumont-Lagacé, S. Lemieux, and C. Perreault. 2013. Transcriptome sequencing of neonatal thymic epithelial cells. *Sci. Rep.* 3: 1860.
44. Balmer, J. E., and R. Blomhoff. 2002. Gene expression regulation by retinoic acid. *J. Lipid Res.* 43: 1773–1808.
45. Ribeiro, A. R., P. M. Rodrigues, C. Meireles, J. P. Di Santo, and N. L. Alves. 2013. Thymocyte selection regulates the homeostasis of IL-7–expressing thymic cortical epithelial cells in vivo. *J. Immunol.* 191: 1200–1209.
46. Jijon, H. B., L. Suarez-Lopez, O. E. Diaz, S. Das, J. De Calisto, M. B. Yaffe, M. J. Pittet, J. R. Mora, Y. Belkaid, R. J. Xavier, and E. J. Villablanca. 2017. Intestinal epithelial cell-specific RARα depletion results in aberrant epithelial cell homeostasis and underdeveloped immune system. *Mucosal Immunol.* DOI: 10.1038/mi.2017.91.
47. Lee, P. P., M. T. Lee, K. M. Darcy, K. Shudo, and M. M. Ip. 1995. Modulation of normal mammary epithelial cell proliferation, morphogenesis, and functional differentiation by retinoids: a comparison of the retinobenzoic acid derivative RE80 with retinoic acid. *Endocrinology* 136: 1707–1717.
48. Agarwal, C., R. A. Chandraratna, M. Teng, S. Nagpal, E. A. Rorke, and R. L. Eckert. 1996. Differential regulation of human ectocervical epithelial cell line proliferation and differentiation by retinoid X receptor- and retinoic acid receptor-specific retinoids. *Cell Growth Differ.* 7: 521–530.
49. Ohigashi, I., S. Zuklys, M. Sakata, C. E. Mayer, Y. Hamazaki, N. Minato, G. A. Hollander, and Y. Takahama. 2015. Adult thymic medullary epithelium is maintained and regenerated by lineage-restricted cells rather than bipotent progenitors. *Cell Rep.* 13: 1432–1443.
50. Paschaki, M., S. C. Lin, R. L. Wong, R. H. Finnell, P. Dollé, and K. Niederreither. 2012. Retinoic acid-dependent signaling pathways and lineage events in the developing mouse spinal cord. *PLoS One* 7: e32447.
51. Koch, U., E. Fiorini, R. Benedito, V. Besseyrias, K. Schuster-Gossler, M. Pierres, N. R. Manley, A. Duarte, H. R. Macdonald, and F. Radtke. 2008. Delta-like 4 is the essential, nonredundant ligand for Notch1 during thymic T cell lineage commitment. *J. Exp. Med.* 205: 2515–2523.
52. Masuyama, N., K. Oishi, Y. Mori, T. Ueno, Y. Takahama, and Y. Gotoh. 2001. Akt inhibits the orphan nuclear receptor Nur77 and T-cell apoptosis. *J. Biol. Chem.* 276: 32799–32805.